Progress In Electromagnetics Research M, Vol. 81, 181–192, 2019

Multi-Objective Optimization Design of Magnetic Bearing Based on Genetic Particle Swarm Optimization

Yukun Sun[1, 2], Shengjing Yin[2], Ye Yuan[2, *], Yonghong Huang[2], and Fan Yang[2]

Abstract—The performance of magnetic bearing is determined by its electromagnetic parameters and mechanical parameters. In order to improve the performance of hybrid magnetic bearing (HMB) to better meet the engineering requirements, which needs to be optimized, a multi-objective optimization method based on genetic particle swarm optimization algorithm (GAPSO) is proposed in this paper to solve the problem that the optimization objectives are not coordinated during the optimization design. By introducing the working principle of HMB, a mathematical model of suspension force is established, and its rationality is verified by the finite-element method. By optimization, the suspension force of the HMB is increased by 18.5%, and the volume is reduced by 22%. The optimization results show that the multi-objective optimization algorithm based on GAPSO can effectively improve the performance of HMB.

1. INTRODUCTION

Magnetic suspension bearing is a new type of support technology that uses non-contact magnetic force to stably suspend the rotor, and it has the advantages of no mechanical contact, no friction, no lubrication, long life, etc. [1–3]. It is widely used in satellite attitude control, flywheel energy storage [4, 5], aerospace, high-speed machine tools, and vacuum ultra-clean [6].

With the development of high-speed, ultra-high-speed technology, the requirements for magnetic bearing technology continue to increase. The main performance indexes of magnetic bearings are bearing capacity, control stiffness, and damping coefficient [7]. The bearing capacity of a magnetic bearing refers to the suspension force under the maximum allowable magnetomotive force, which depends on the structural parameters of the magnetic bearing. The larger the volume of the magnetic bearing is, the longer the axial length can produce the greater suspension force. However, with the increase of the volume, the loss of the magnetic bearing will also increase. And the increase of the axial length leads to the decrease of the critical speed of the rotor and the increase of the wind wear loss [8]. Therefore, in order to improve the performance of the magnetic bearing, the structural parameters should be optimized.

The traditional optimization method mainly uses single-objective optimization by finite element software, in which calculation amount is large, and it is difficult to obtain an optimal solution for the mutual influence of each objective. In [9–11], magnetic bearings were optimized for single-objective optimization with volume, suspension force, and loss, respectively. Better results for single objective were obtained, but the other performance of the magnetic bearing was degraded. In [12], the Taguchi optimization method is proposed, which can greatly reduce the amount of simulation calculation, but the selection of its optimal value has certain limitations. The multi-objective evolutionary algorithm MOEAS is used to optimize the axial hybrid magnetic bearing with biased permanent magnets in [13].

Received 19 March 2019, Accepted 5 June 2019, Scheduled 13 June 2019

* Corresponding author: Ye Yuan (763874383@qq.com).

[1] School of Power Engineering, Nanjing Institute of Technology, Nanjing 211167, China. [2] School of Electrical and Information Engineering, Jiangsu University, Zhenjiang 212013, China.

In [14], the particle swarm optimization method was used to optimize radial magnetic bearings with volume and loss as optimization objectives, which obtained better optimization results. However, the above several optimization algorithms still use global optimization, which is easy to fall into local optimum in the optimization process, and the optimization efficiency is low. Therefore, it is necessary to find a fast convergence and global optimization algorithm for the design of MB. The GAPSO is an optimization algorithm which combines genetic algorithm with particle swarm optimization. The algorithm has the advantages of strong global search ability, strong local search ability, fast convergence speed, and high running speed.

The mathematical model of the magnetic bearing is established by the equal magnetic circuit method based on the analysis of the working principle in this paper. The Ansys Maxwell finite element simulation model is established based on initial parameters, and the correctness of the mathematical model is verified. Finally, the GAPSO is used to optimize with the suspension force and volume as the optimization objectives.

2. GENETIC PARTICLE SWARM OPTIMIZATION

Particle Swarm Optimization (PSO) algorithm is proposed by Kennedy and Eberhart in 1995, which is an evolutionary algorithm based on swarm intelligence originates from complex group behavior such as bird foraging [15–17]. The PSO first initializes a random particle swarm, and by calculating the fitness value of all particles, the individual optimal and global optimal values of the current particle are obtained [18]. The updating of the position and velocity of the particles in flight is determined by both the individual and global optimum values, which leads to the continuous updating of the individual and global optimum values of the particle swarm. The optimal solution of the asymptotic problem is approximated, and the optimal solution is finally obtained. The updating formulas of particle velocity and position are as follows [19]:

$$v_{iD}^{k+1} = \omega v_{iD}^{k} + c_1 r_1 \left(p_{iD}^{k} - x_{iD}^{k}\right) + c_2 r_2 \left(p_{gD}^{k} - x_{gD}^{k}\right) \tag{1}$$

$$x_{iD}^{k+1} = x_{iD}^{k} + v_{iD}^{k+1} \tag{2}$$

where i is the particle number; k is the iteration number, c_1 and c_2 are the learning factor; w is the inertia factor; p_i is the current individual optimal position; p_g is the current global optimal position; v_i is the current particle velocity.

The GAPSO is a method that introduces the idea of crossover and mutation into the PSO. This algorithm not only ensures the powerful global search ability of genetic algorithm, but also integrates the position transfer idea of particle swarm. More efficiently, the obtained solution has higher precision and avoids the premature convergence of particle swarm algorithm due to partial deadlock. Several important steps of the GAPSO are as follows:

Step1: Initialize the population, parameter assignment;

Step2: Calculate the fitness value of each particle, obtain the individual optimal value and the global optimal value;

Step3: Update the speed and position of some population particles, select 30% of the population particles for crossover and mutation operation.

Step4: Calculate the fitness value of the effective particles and update the individual optimal and global optimal values.

Step5: If the iteration condition is met, the condition is stopped, and the optimal solution is obtained; otherwise, step 2 is reversed.

3. MODEL OF HYBRID MAGNETIC BEARING

3.1. Structure of Hybrid Magnetic Bearing

The basic structure of hybrid magnetic bearing is shown in Figure 1. It consists of a radial stator, radial control coil, permanent magnet (PM), and rotor. The stator core is made of silicon steel sheets, and

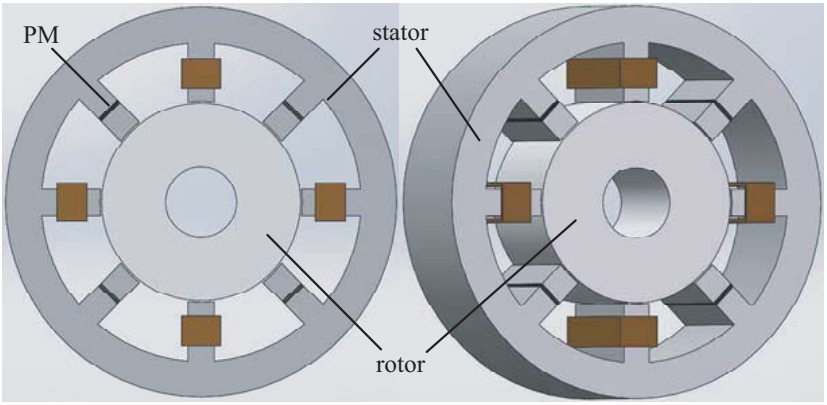

Figure 1. Structure of hybrid magnetic bearing.

the stator is 8 magnetic poles arranged symmetrically in space, four of which are control poles, and the other four poles are PM poles. The PM is made of Nd-Fe-B, used to generate bias flux. In order to reduce hysteresis and eddy current losses, the core of the rotor is also laminated with silicon steel sheets and mounted on a rotating shaft.

3.2. Working Principle of Hybrid Magnetic Bearings

From the magnetic circuit diagram in Figure 2, it can be seen that the bias flux generated by the PM flows through the permanent magnet pole, permanent magnet air gap, rotor core, control air gap, control pole, and stator yoke to form a closed loop (as shown in the solid line in Figure 2). The control winding generates the control flux through the stator yoke, control pole, air gap under the control pole, rotor core, and then closes through the stator yoke (as shown in the dashed line in Figure 2). Since the magnetoresistance of the permanent magnet is large, the control flux does not pass through the permanent magnet pole, and the demagnetization of the permanent magnet by the control flux can be avoided.

The working principle of HMB is that the rotor is in the balance position of suspension under the action of bias magnetic field suction produced by PM. When the rotor core is in the equilibrium position, each PM produces an equal bias magnetic flux at the air gap, and the resultant force is zero.

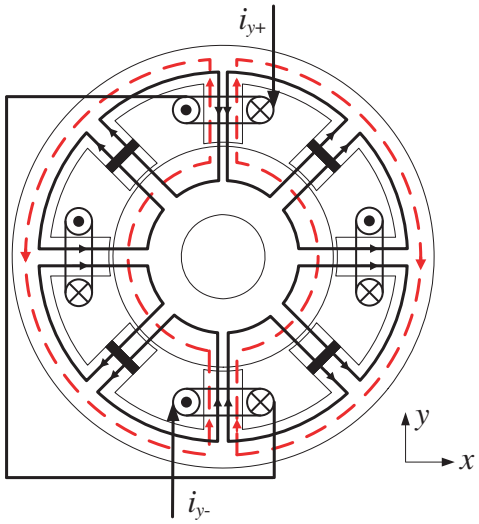

Figure 2. Magnetic circuit of HMB.

Assuming that the core of the rotor is disturbed by a force in the positive direction along the y-axis, the rotor will deviate from the balance position and move upward, resulting in a change in the bias flux of the air gap in the positive and negative directions of the y-axis; the lower part of the x-axis increases; the bias flux decreases; the upper part decreases; and the bias flux increases, which will produce an upward force on the rotor. At this time, the control current of the control winding leads to the control flux. The superposition of the flux and bias flux leads to the decrease of the flux in the positive air gap of the y-axis of the rotor core, and the increase of the flux in the negative air gap of the y-axis, resulting in a negative suction along the y-axis, which pulls the rotor back to the balance position. Similarly, regardless of the external disturbance of the rotor in the negative direction of the y-axis and the positive or negative direction of the x-axis, the above control maintains the rotor in an equilibrium position.

3.3. Mathematical Model of HMB

The magnetic path of HMB consists of a biasing magnetic circuit and a control magnetic circuit. In order to simplify the calculation of the magnetic circuit, the magnetic circuit of the HMB is assumed as follows: only the magnetic leakage of the inner and outer surfaces of the permanent magnet is considered, and the bias magnetic flux is provided by the PM. Only the working air gap reluctance is considered, while the core magnetic resistance, rotor magnetic resistance, and eddy current loss are neglected. The equivalent magnetic circuits of bias magnetic circuit and control magnetic circuit of HMB are shown in Figures 3(a) and (b), where F_m is the magnetomotive force of PM; Ni is the magnetomotive forces generated by coils in y-axis; ϕ_{p1}, ϕ_{p2}, ϕ_{p3}, and ϕ_{p4} are the magnetic flux generated in the air gap of the permanent magnet in the x, y directions; ϕ_{c1}, ϕ_{c2}, ϕ_{c3}, and ϕ_{c4} are the control flux generated by the control winding; G_{c1}, G_{c2}, G_{c3}, and G_{c4} are the air gap permeability in the x, y directions; G_{m1}, G_{m2}, G_{m3}, and G_{m4} are the permeability at the permanent magnetic pole air gap. Assume that the rotor deviates away from the equilibrium position and that the radial displacements in y-axis is y. The permeability at the air gap in the x and y directions can be calculate as

$$\begin{cases} G_{c1} = \dfrac{\mu_0 S}{g_0 - y} \\ G_{c2} = \dfrac{\mu_0 S}{g_0} \\ G_{c3} = \dfrac{\mu_0 S}{g_0 + y} \\ G_{c4} = \dfrac{\mu_0 S}{g_0} \end{cases} \tag{3}$$

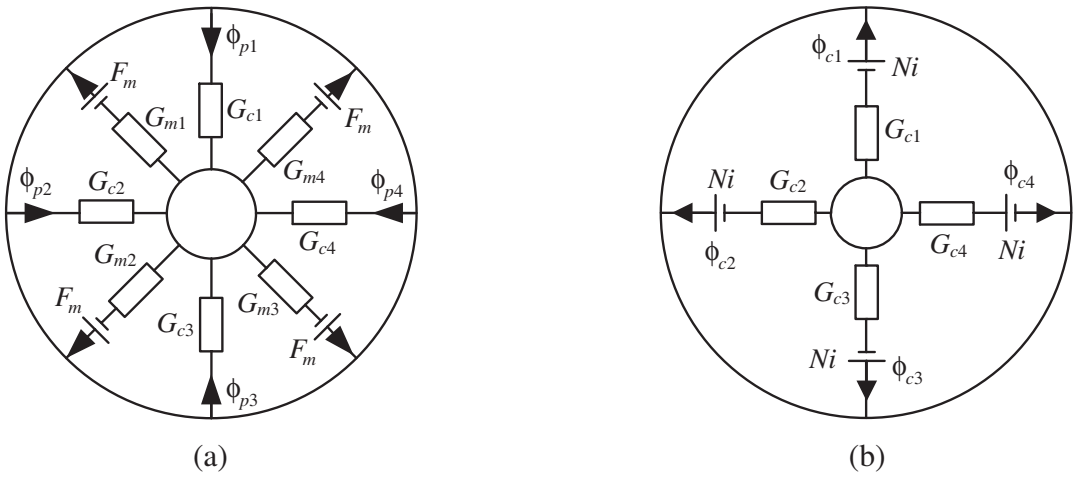

Figure 3. Equivalent magnetic circuit of HMB. (a) Bias magnetic flux path. (b) Control flux paths.

Permeability at the permanent magnetic pole air gap:

$$\begin{cases} G_{m1} = G_{m4} = \dfrac{\mu_0 S}{g_0 - y\cos\theta} \\ G_{m2} = G_{m3} = \dfrac{\mu_0 S}{g_0 + y\cos\theta} \end{cases} \tag{4}$$

where g_0 is the lengths of the air-gaps, μ_0 the permeability in vacuum, and S the areas of radial magnetic pole faces. As the demagnetization curve of PM can be approximated by a straight line, the equations can be obtained as $F_m = H_c h_m$, where h_m is the thickness of permanent magnet and H_c the coercive force of PM. Based on the equivalent magnetic circuit diagram and Kirchhoff's law, the magnetic circuit equation can be obtained as

$$\begin{cases} \phi_{p1} = \dfrac{F_m(G_{m1}+G_{m2}+G_{m3}+G_{m4})G_{c1}}{(G_{m1}+G_{m2}+G_{m3}+G_{m4}+G_{c1}+G_{c2}+G_{c3}+G_{c4})} \\ \phi_{p3} = \dfrac{F_m(G_{m1}+G_{m2}+G_{m3}+G_{m4})G_{c3}}{(G_{m1}+G_{m2}+G_{m3}+G_{m4}+G_{c1}+G_{c2}+G_{c3}+G_{c4})} \\ \phi_{c1} = \phi_{c3} = \dfrac{Ni\mu_0 S}{g_0} \end{cases} \tag{5}$$

In order to return to the equilibrium position, the synthesized flux at the air gap must produce a downward resultant force F_y. Based on the relationship between the magnetic field force and magnetic flux, the suspension force F_y in the y-axis direction can be obtained as

$$F_y = \frac{1}{2\mu_0 S}\left[(\phi_{p3}+\phi_{c3})^2 - (\phi_{p1}-\phi_{c1})^2\right] \tag{6}$$

By using Taylor's formula to linearize the F_y, the linearization equation of the rotor near the equilibrium position can be obtained as follows:

$$F_y \approx \frac{\partial F_y}{\partial y}y + \frac{\partial F_y}{\partial y}i_y = k_y y + k_i i_y \tag{7}$$

where k_y and k_i are the force-current stiffness and force-displacement stiffness, respectively, near the equilibrium position in y direction. The expressions of both are

$$k_y = -\frac{F_m^2 \mu_0 S\left(1+2\cos^2\theta\right)}{4g_0^3} \tag{8}$$

$$k_i = \frac{F_m N \mu_0 S}{g_0^2} \tag{9}$$

4. DESIGN AND ANALYSIS OF HMB

According to the design formula of magnetic bearing parameters in [20–22] and the requirements of practical application, the initial model parameters of the magnetic bearing designed in this paper are shown in Table 1.

In this paper, the suspension force of the HMB with different rotor displacements and different control currents are calculated by 3D finite-element method and analytical method. By comparing the results of the above mathematical model, the rationality of optimizing the bearing by analytical model is demonstrated. Figure 4 shows the suspension force curves obtained by finite element method and analytical method under different control currents. In Figure 4, when the control current is -4 to 4 A, the error calculated by the finite element method and analytical method is less than 3%, and the suspension force is linear with the control current.

The relationship between the displacement and the suspension force obtained by the finite element method and analytical method under different rotor displacements is show in Figure 5. When the rotor is displaced, the suspension force error calculated by the finite element method and analytical method is between 2% and 10%.

Table 1. Initial parameter values.

Parameter	Value
Outer radius of stator/r_5	55 mm
Inner radius of stator/r_4	46 mm
Outer radius of rotor/r_2	28 mm
Inner radius of rotor r_1	10 mm
Coil number	40
The Axial length/l	40 mm
The Air gap length/g_0	0.5 mm
The thickness of PM/h_m	2 mm

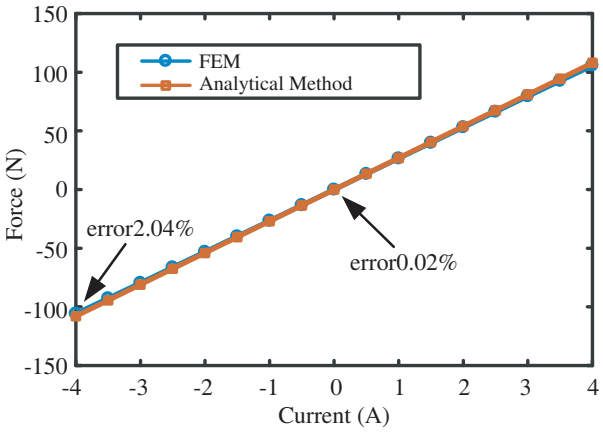

Figure 4. Current-force relationship.

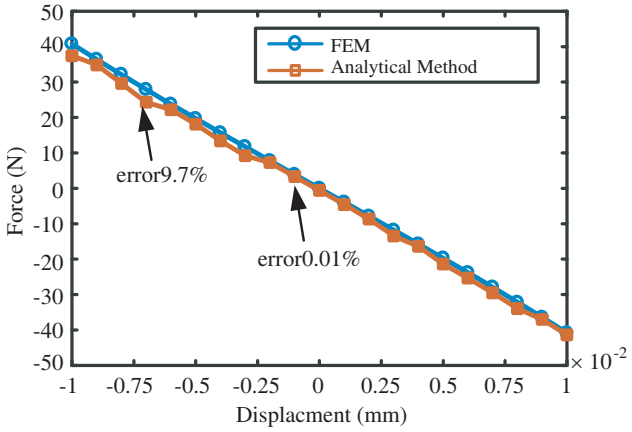

Figure 5. Displacement-force relationship.

The relative error rates above show good consistency of the curves obtained by the finite element method and analytical method. It can be observed form the curves that the suspension force is proportional to the control current and also proportional to the displacement of the rotor in the equilibrium position under the condition of unsaturated iron core.

5. OPTIMIZATION OF HMB

Through the analysis of magnetic bearing, this section carries out multi-objective optimization of HMB. The optimization process is shown in Figure 6: (1) Determine the optimization objectives, design variables, and constraints. (2) The objective function, design variables and constraints are brought into the algorithm to obtain the optimal solution. (3) To verify the optimization results by using the finite element.

5.1. GAPSO Optimization Design

The HMB mainly provides controllable suspension force for the rotor, so that the rotor can withstand external disturbances and stably suspend in the balanced position, and the suspension force provided by magnetic bearings should be as large as possible. The magnitude of the suspension force is determined not only by the structural parameters of the bearing, but also by the control current. The maximum suspension force provided by magnetic bearing should be the state when the flux density of stator pole reaches the saturated flux density of material. The objective function of suspension force can be

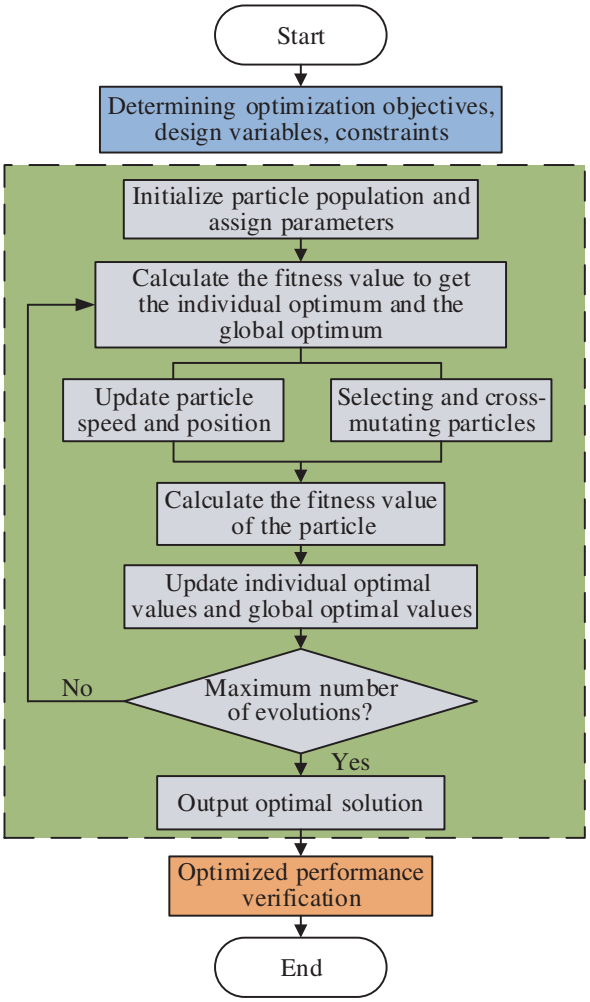

Figure 6. Multi-objective optimization steps.

expressed as

$$\begin{cases} F_y = \dfrac{1}{2\mu_0 S}\left[(\phi_{p3}+\phi_{c3})^2 - (\phi_{p1}-\phi_{c1})^2\right] \\ \phi_{p3}+\phi_{c3} < B_s S \end{cases} \tag{10}$$

Substituting Eq. (5) into Eq. (6), the formula of the maximum suspension force is expressed as:

$$\max F = \frac{F_m^2 S \mu_0}{2g_0^2} \tag{11}$$

Considering the cost and actual application environment, the volume and axial length of the magnetic bearing should be as small as possible. Therefore, the volume of the magnetic bearing is taken as the optimization target. The total volume can be expressed as

$$V = V_r + V_s + V_{pm} \tag{12}$$

where V_r is the volume of the HMB, V_s the volume of the stator, and V_{pm} the volume of the PM.

The design variables of the HMB are shown in Figure 7, where r_5, r_4, r_3, r_2, r_1, g_0, θ, and l are design variables. Because the rotor is rigid, the internal diameter of the rotor is obtained by modal calculation. r_3 can be expressed by the rotor outer diameter r_2 and air gap g_0, so r_1 and r_3 are not as design variables. Considering the operation characteristics and manufacturing process of magnetic bearings, the length of air gap should not be too small, so g_0 is usually taken as 0.3 to 0.8. According

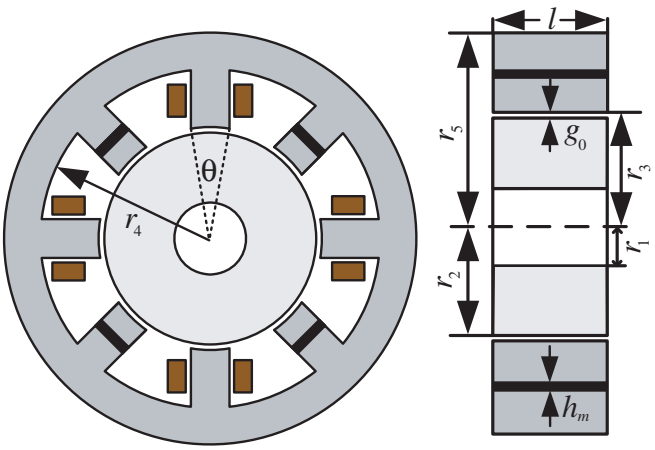

Figure 7. Design variables of HMB.

to the design experience and geometric rules and considering the actual application environment, the constraints of design variables are as follows

$$\begin{cases} r_5 - r_4 > 0 \\ r_4 - r_3 > 0 \\ r_3 - r_2 > 0 \\ r_2 - r_1 > 0 \\ r_4 - r_2 - g_0 > 0 \end{cases} \tag{13}$$

Another constraint for magnetic bearings in design optimization is flux density [14, 22]. The saturated flux density of soft-magnetic materials is 1.6 T. In order to avoid the saturation of soft magnetic materials, the air gap flux density is limited to 1.2 T. The air gap flux includes control flux and bias flux. When suspension force reaches the maximum, the density of control flux and bias flux is 0.6 T, respectively. So the constraints of flux density are as follows

$$\begin{cases} B_c \leq 0.6 \\ B_0 \leq 0.6 \\ B_{\max} \leq 1.2 \end{cases} \tag{14}$$

5.2. Analysis of Optimization Results

After determining the optimization objective function, design variables and constraints, the main parameters of the GAPSO are set: the population size is 1000; the number of iterations of the particles is 10; and the acceleration coefficients c_1 and c_2 are both 2. After 10 iterations, the Pareto optimal solution is shown in Figure 8. Each point in the graph corresponds to an optimal solution.

By analyzing the optimization results and combining with the actual situation, this paper chooses a optimal solutions as the optimization results from the Pareto optimal solution front shown in Figure 9. The results of design variables and optimization objectives of initial design and GAPSO design are shown in Table 2.

From the data in Table 2, the performance of the HMB has been greatly improved by the GAPSO; the volume decreases from 2.534E-4 m^3 to 1.976E-4 m^3 with the rate 22%; the axial length decreases from 40 mm to 36 mm, a decrease of 10%; the suspension force increases from 105N to 128.8N, an increase of 18.5%. In order to verify the correctness and effectiveness of GAPSO, the distribution of magnetic flux density of HMB is calculated by finite element method. Figure 11 shows the magnetic density map of the bias magnetic fluxes before and after optimization. From Figure 10, the bias magnetic flux density in the air gap before optimization is about 0.5 T, and that in the optimized air gap is about 0.6 T.

The distribution of magnetic flux density of HMB of initial design and the GAPSO design with maximum control current are shown in Figure 11. The maximum magnetic flux density of initial design

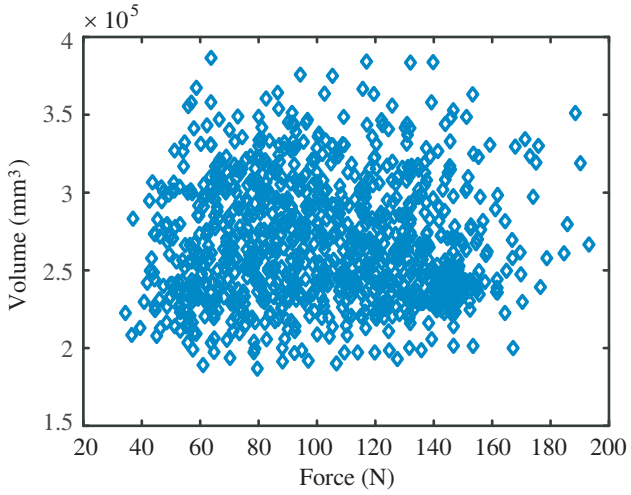

Figure 8. Pareto optimal solution.

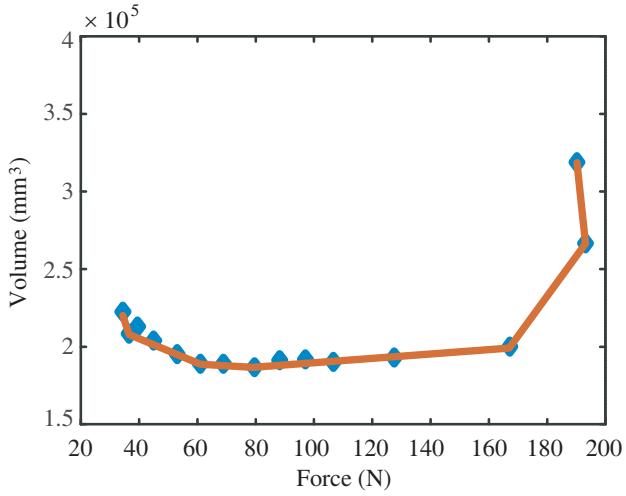

Figure 9. Pareto optimal front.

Table 2. GAPSO optimization results.

Parameter	Initial design	GAPSO
r_5	55 mm	50 mm
r_4	46 mm	41.3 mm
r_2	28 mm	26.7 mm
g_0	0.5 mm	0.5 mm
h_m	2 mm	2.2 mm
l	40 mm	36 mm
θ	15	19.5
F	105N	128.8N
V	2.534E-4 m^3	1.976E-4 m^3

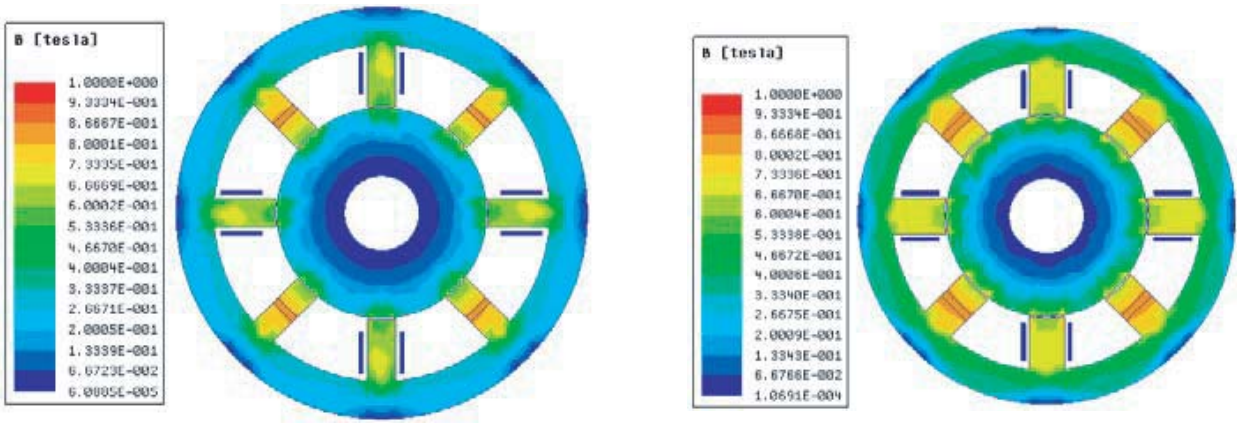

(a) (b)

Figure 10. Distribution of bias magnetic flux density. (a) Initial design. (b) GAPSO design.

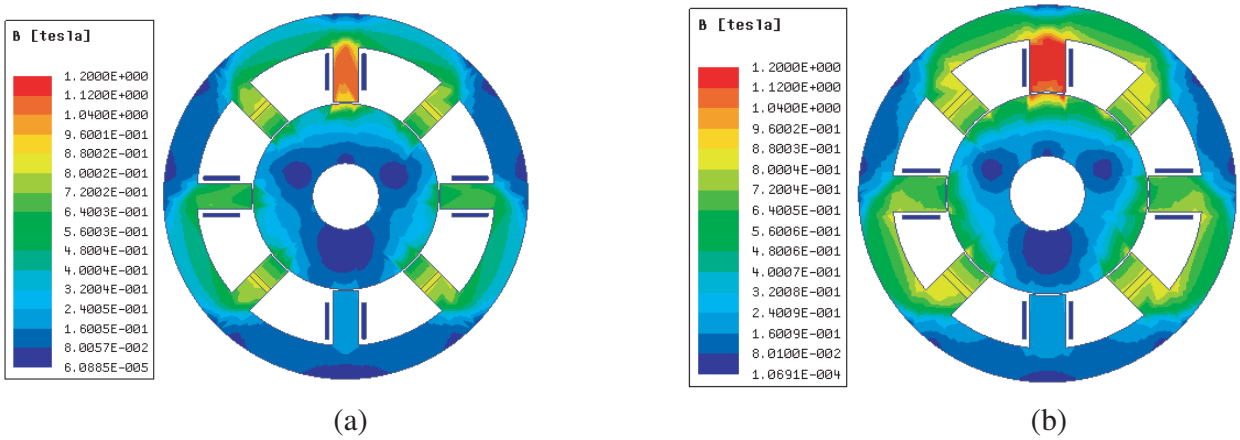

Figure 11. Distribution of magnetic flux density with maximum control current. (a) Initial design. (b) GAPSO design.

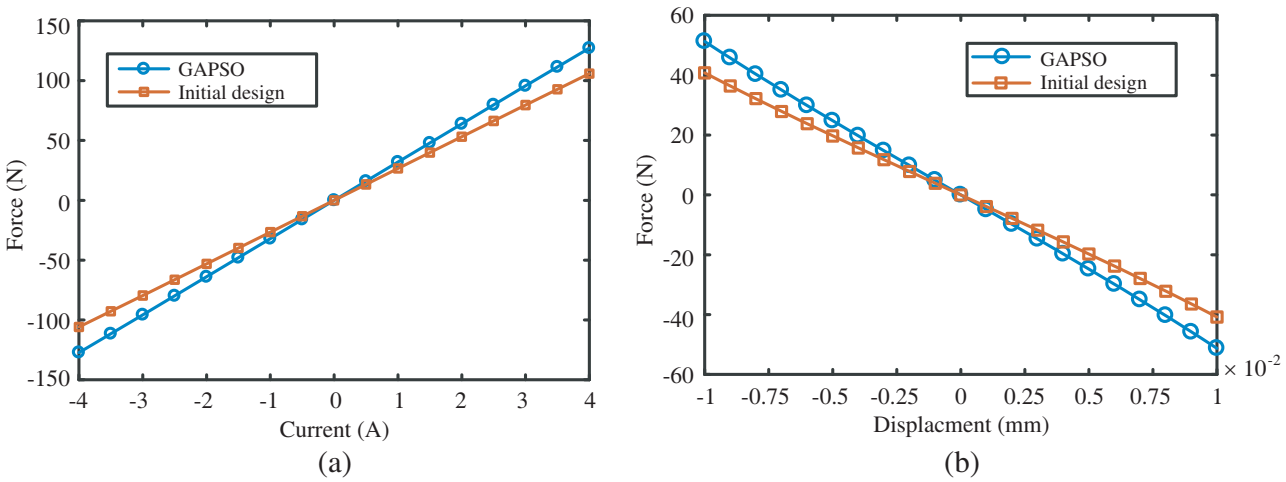

Figure 12. Current/displacement-force of initial design and GAPSO design. (a) Current-force relationship. (b) Displacement-force relationship.

in air-gaps is about 1.0 T, while the magnetic flux density of GAPSO design is optimized at about 1.1 T in air-gaps, which is less than the saturated flux density of soft-magnetic material 1.6 T.

The comparison of the suspension force of the HMB of initial design and the GAPSO design with the rotor displacement and control current is shown in Figure 12. The suspension force is proportional to the rotor displacement and control current, and current stiffness and displacement stiffness of the optimized magnetic bearing increase. For the same load, the larger the displacement stiffness is, the smaller the displacement of the rotor is from the equilibrium position. The better the dynamic response of the HMB is, the smaller the current is required for the current stiffness. Therefore, the optimized magnetic bearing has better performance than that before optimization.

6. CONCLUSION

In this paper, design and parameter optimization of the HMB is studied. The mathematical model of HMB is established by using equivalent magnetic circuit method, and its rationality is verified by finite element method. Then multi-objective optimization design of suspension force and volume is carried out by GAPSO. The optimization results show that the suspension force of the HMB is improved by 18.5%, and the volume is reduced by 22%. The performance of the magnetic bearing is greatly

improved compared with the initial design. Compared with the finite element method, the GAPSO used in this paper has higher optimization efficiency, which has certain theoretical significance and engineering practical value.

ACKNOWLEDGMENT

This work was sponsored by the National Natural Science Foundation of China (51877101, 51707082) Natural Science Foundation of Jiangsu Province (BK20170546) and Priority Academic Program Development of Jiangsu Higher Education Institutions.

REFERENCES

1. Huang, Z., J. Fang, X. Liu, et al., "Loss calculation and thermal analysis of rotors supported by active magnetic bearings for high-speed permanent-magnet electrical machines," *IEEE Transactions on Industrial Electronics*, Vol. 63, No. 4, 2027–2035, 2016.
2. Santra, T., D. Roy, A. B. Choudhury, and S. Yamada, "Vibration control of a hybrid magnetic bearing using an adaptive sliding mode technique," *Journal of Vibration and Control*, Vol. 24, No. 10, 1848–1860, 2018.
3. Santra, T., D. Roy, and A. B. Choudhury, "Calculation of passive magnetic force in a radial magnetic bearing using general division approach," *Progress In Electromagnetics Research M*, Vol. 54, 91–102, 2017.
4. Han, B., S. Zheng, X. Wang, et al., "Integral design and analysis of passive magnetic bearing and active radial magnetic bearing for agile satellite application," *IEEE Transactions on Magnetics*, Vol. 48, No. 6, 1959–1966, 2012.
5. Nguyen, T. D. and G. Foo, "Sensorless control of a dual-airgap axial flux permanent magnet machine for flywheel energy storage system," *IET Electric Power Applications*, Vol. 7, No. 2, 140–149, 2013.
6. Han, B., S. Zheng, Y. Le, et al., "Modeling and analysis of coupling performance between passive magnetic bearing and hybrid magnetic radial bearing for magnetically suspended flywheel," *IEEE Transactions on Magnetics*, Vol. 49, No. 10, 5356–5370, 2013.
7. Wang, X., D. Zhang, P. Gao, et al., "Structural optimization design of radial magnetic bearing for flywheel energy storage," *Mechanical Science and Technology*, Vol. 37, No. 7, 1048–1054, 2018.
8. Mitterhofer, H., W. Gruber, and W. Amrhein, "On the high speed capacity of bearingless drives," *IEEE Transactions on Industrial Electronics*, Vol. 61, No. 6, 3119–3126, 2014.
9. Moser, R., J. Sandtner, and H. Bleuler, "Optimization of repulsive passive magnetic bearings," *IEEE Transactions on Magnetics*, Vol. 42, No. 8, 2038–2042, 2006.
10. Zeisberger, M., T. Habisreuther, D. Litzkendorf, et al., "Optimization of levitation forces in superconducting magnetic bearings," *IEEE Transactions on Applied Superconductivity*, Vol. 11, No. 1, 1741–1744, 2001.
11. Sahinkaya, M. N. and A. E. Hartavi, "Variable bias current in magnetic bearings for energy optimization," *IEEE Transactions on Magnetics*, Vol. 43, No. 3, 1052–1060, 2007.
12. Lan, Z., X. Yang, F. Wang, et al., "Application for optimal designing of sinusoidal interior permanent magnet synchronous motor by using the Taguchi method," *Transactions of China Electrotechnical Society*, Vol. 26, No. 12, 37–42, 2011.
13. Rao, J. S. and R. Tiwari, "Optimum design and analysis of axial hybrid magnetic bearings using multi-objective genetic algorithms," *International Journal for Computational Methods in Engineering Science & Mechanics*, 10–27, 2012.
14. Liu, X. and B. Han, "The multiobjective optimal design of a two-degree-of-freedom hybrid magnetic bearing," *IEEE Transactions on Magnetics*, Vol. 50, No. 9, 1–14, 2014.
15. Han, B., Q. Xu, and Q. Yuan, "Multiobjective optimization of a combined radial-axial magnetic bearing for magnetically suspended compressor," *IEEE Transactions on Industrial Electronics*, Vol. 63, No. 4, 2284–2293, 2016.

16. Kennedy, J. and R. Eberhaa, "Particle swarm optimization," *IEEE Int. Confon. Neural Networks*, 1942—1948, IEEE, Perth, USA, 1995.
17. Zhang, Y., D. Gong, and Y. Jiang, "Barebones particle swarm for multi-objective optimization problems," *International Journal of Innovative Computing & Applications*, Vol. 2, No. 2, 86–99, 2009.
18. Trelea, I. C., "The particle swarm optimization algorithm: Convergence analysis and parameter selection," *Information Processing Letters*, Vol. 85, No. 6, 317–325, 2003.
19. Eberhart, R. and J. Kennedy, "A new optimizer using particle swarm theory," *Proceedings of the 16th International Symposium on Micro Machine and Human Science*, 39–43, Nagoya, Japan, 1995.
20. Zhao, X., Z. Deng, and B. Wang, "Parameter design and realization of permanent magnet biased heterploar radial magnetic bearing," *Transactions of China Electrotechnical Society*, Vol. 27, No. 7, 131–138, 2012.
21. Zhu, H., Z. Deng, S. Yuan, et al., "The working principle and parameter design permanent magnet biased radial-axial direction magnetic bearing," *Proceedings of the CSEE*, Vol. 22, No. 9, 54–58, 2002.
22. Fang, J., C. Wang, and T. Wen, "Design and optimization of a radial hybrid magnetic bearing with separate poles for magnetically suspended inertially stabilized platform," *IEEE Transactions on Magnetics*, Vol. 50, No. 5, 1–11, 2014.